論文 / 著書情報
Article / Book Information

Title	ANALYSIS OF FLOW CONTROL VALVE IN HYDRAULIC SYSTEM USING PARTICLE EXCITATION
Authors	Takahiro UKIDA, Koichi SUZUMORI, Hiroyuki NABAE, Takefumi KANDA
Citation	The 10th JFPS International Symposium on Fluid Power
Pub. date	2017, 10

ANALYSIS OF FLOW CONTROL VALVE IN HYDRAULIC SYSTEM USING PARTICLE EXCITATION

Takahiro UKIDA*, Koichi SUZUMORI**, Hiroyuki NABAE**, Takefumi KANDA***

* Department of Mechanical and Aerospace Engineering, Graduate School of Science and Engineering, Tokyo Institute of Technology
2-12-1 Ookayama, Meguro-ku, Tokyo, 152-8552 Japan
(E-mail: ukida.t.ab@m.titech.ac.jp)
** School of Engineering, Tokyo Institute of Technology
2-12-1 Ookayama, Meguro-ku, Tokyo, 152-8552 Japan
*** Graduate School of Natural Science and Technology, Okayama University
3-1-1 Tsusima-naka, Kita-ku, Okayama, 700-8530 Japan

Abstract. In this paper, we attempted to clarify the driving condition of the flow control valve in hydraulics system using the particle excitation. A new analytical model was proposed to reveal the characteristics of the valve and the effect of the viscosity of the working fluid. It was examined the open state of the valve under several assumptions including the assumption of Reynolds equation, focusing on the movement of the particles near the orifices and the flow of the working fluid in the narrow flow path. The results of the analysis were compared with the experimental results. The analytical results indicated that the proposed model represents the open state of the valve in the low viscosity hydraulic oil.

Keywords: Proportional Control Valve, Hydraulics, Flow Control, Piezoelectric Element.

INTRODUCTION

Mobile robots driven by hydraulic actuators have the possibility to evolve into “tough robots” which are resistant to impacts from the external environment and can generate a large force [1–3]. Mobile robots comprise hydraulic actuators equipped with a large number of two-stage servo valves to control complex behaviors with multiple degrees of freedom. Compared to direct drive servo valves, two-stage servo valves are smaller and have high responsiveness [4], which makes them suitable for use in hydraulic actuator based mobile robots. However, two-stage servo valves have a complex structure and cost disadvantage.

In order to mitigate these disadvantages, we have developed a small, PZT driven flow control valve with a simple structure [5]. This valve was originally developed as a flow control valve for pneumatic systems [6, 7]. The orifices of the valve are sealed by the particles confined in the valve. They open and close because of the excitation of particles caused by the vibration of the orifice plate and fluid force; this results in a simple and compact structure. The open condition of the orifices is that the particles gain inertia above the pressing force due to differential pressure between the inlet of the valve and the outlet of the valve. However, when the viscous fluid is used as the working fluid, the effective flow does not occur unless the particles do not gain larger inertia than the above condition. Furthermore, the pressure generated by squeeze effect between the particles and the valve seat of the orifices prevents the movement of the particle. As a result, the flow path keeps narrow. This phenomenon also makes the working fluid hard to flow.

In this paper, we propose a new analytical model focusing on the flow between the particles and the valve seat of the orifices to reveal the characteristics of the valve and the effect of the viscosity of the working fluid. To evaluate the proposed model, the results of numerical simulation is compared with experimental results.

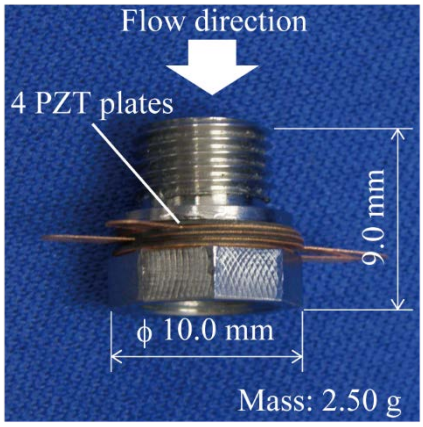

FIGURE 1. Photograph of the valve.

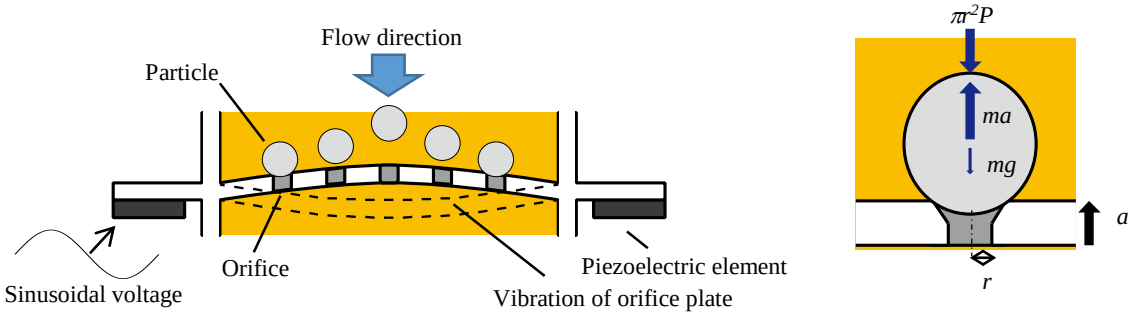

(a) Cross sectional view of the schematics

(b) Forces acting on the particle. The direction of gravity is downward in the figure.

FIGURE 2. Working principle of the valve using particle excitation.

PRINCIPLE OF THE PARTICLE EXCITATION VALVE

Figure 1 and 2 show a photograph and a working principle of a particle-excitation flow control valve, respectively. The valve consists of the orifice plate, upon which multiple orifices have been arranged; particles, and piezoelectric elements, which are 0.2-mm-thick ring-shaped lead zirconate titanate (PZT). When this valve is not in operation, the particles which is carried onto the orifices by fluid force seal the orifices. The valve is the closed state at this time. When a sinusoidal voltage is applied to piezoelectric elements, the valve changes into the open state. The piezoelectric elements which the sinusoidal voltage is applied to at resonant frequency vibrate the orifice parts. The particles which gain the inertia by the vibration of the orifice parts separate from the orifices. This principle results in a simple and compact structure.

The condition that the particles separate from orifices is derived from the balance force acting on the particle [6].

$$a_o > \frac{\pi r_o^2 P_s \pm mg}{m} \tag{1}$$

Where a_o is the acceleration of the valve seat at the orifice part, P_s is supply pressure, r_o is the radius of the orifice, m is the mass of the particle, and g is the acceleration due to gravity.

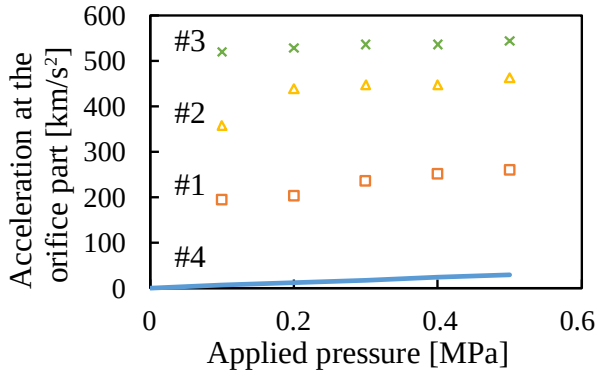

FIGURE 3. Relationship between the applied pressure and the acceleration to open the orifice. #1, #2, and #3 represent the experimental results, where silicone oils are used as the working fluid with kinematic viscosity values 1, 3, and 5 mm^2/s, respectively. #4 represents the value derived by Eq. (1).

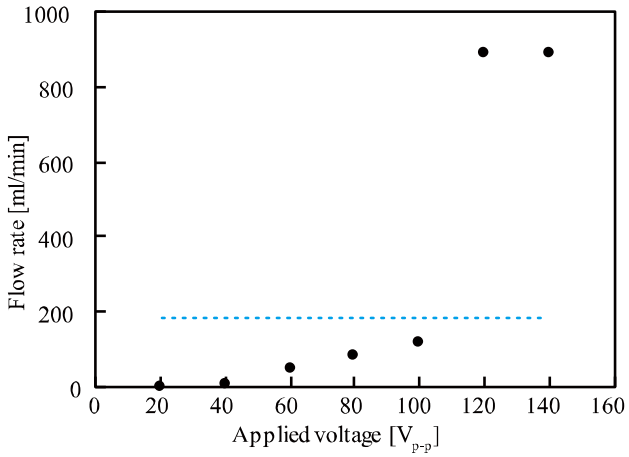

FIGURE 4. Relationship between the flow rate and the applied voltage with the applied pressure of 0.5 MPa. The dashed line shows the maximum flow rate per an orifice with same applied pressure.

MODELING OF THE PARTICLE EXCITTATION VALVE IN HYDRAULICS

When the valve is applied to hydraulics, for the valve to actually start operation, it is necessary that the acceleration at the orifices greatly exceeds the lower limit value of the acceleration obtained from Eq. (1). Figure 3 shows the acceleration of the orifice part at which the valve begin operations obtained from Eq. (1) and that obtained through experiments. Note that we defined the control valve stably opens, when the flow rate exceeded 5 ml/min. The experiment was conducted using silicone oil as the working fluid. The result indicates that the viscosity of the working fluid affects the driving of the valve. This fact shows necessity of an analytical model to clarify the effect of viscosity to the valve operation. This section discusses a modeling method for representing the phenomena under the valve operation.

Assumptions for modeling

Figure 4 shows the relationship between the flow rate and the applied voltage with the applied pressure of 0.5 MPa and the ability to flow per one orifice, when silicone oil with kinematic viscosity of 1 mm^2/s is used as the working fluid. When the applied voltage was 120 $V_{p\text{-}p}$ or more, not only was the flow rate of the valve higher than the maximum flow rate per one orifice, it was also saturated because all particles were sufficiently separated from all orifices. On the other hand, when the applied voltage was 100 $V_{p\text{-}p}$ or less, the flow rate of the valve was less than the maximum flow rate per one orifice. The results predict that the particles are near the orifices and repeatedly opening and closing them, in sequence. Therefore, we examine the open state of the valve under the following assumptions, focusing on the movement of the particles near the orifices and the flow of the working fluid in the narrow flow path.

(i) When the flow path is narrow, the pressure of the chamber in the valve does not reduce.
(ii) The fluid between the particles and the valve seat of the orifices has the assumption of the Reynolds equation.
(iii) The relationship between the particles and the valve seat of the orifices are regarded as a parallel plate.
(iv) The particles separating from the orifices move on the vertical direction axis of the orifices.
(v) The valve seat moves on the vertical direction axis of the orifices.
(vi) The flow between the particles and the valve seat of the orifices is axisymmetric.
(vii) The collision between particles and the orifices does not affect the vibration of the orifice plate.

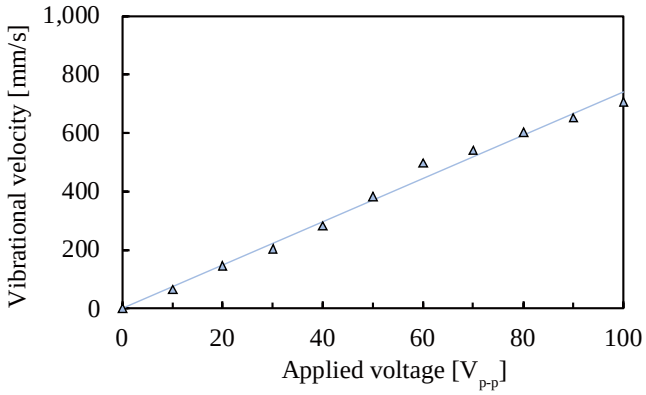

FIGURE 5. Relationship between vibrational velocity at the central part of the orifice plate and the applied voltage, where the silicone oil is used as the working fluid with kinematic viscosity value 1 mm^2/s.

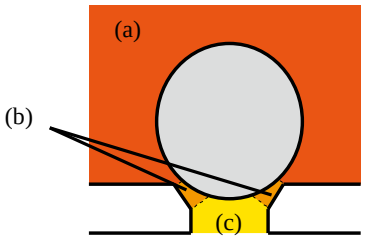

FIGURE 6. Pressure distribution around the particle.

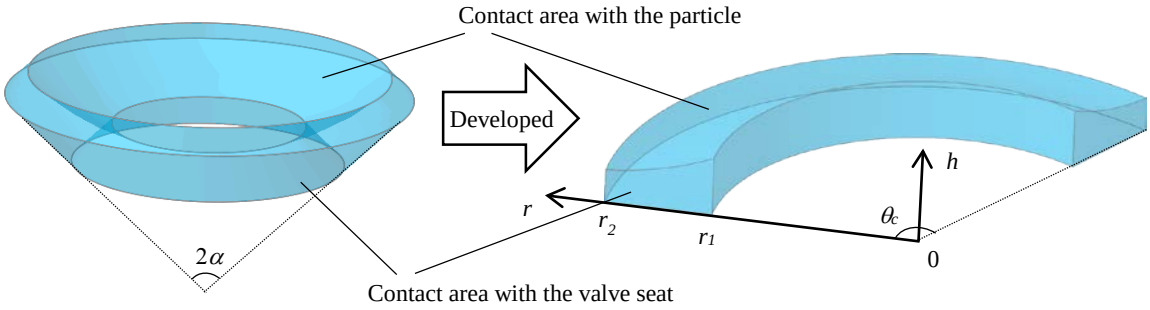

FIGURE 7. Developed view of the flow path between the particle and the valve seat.

Movement of the particles

The movement of the particle separated from valve seat is obtained from initial velocity of the particle, the forces acting on the particle, and a coefficient of restitution between the particle and the valve seat. The initial velocity of the particle is obtained from the vibrational velocity of the orifice plate. As shown in figure 5, the relationship between the vibrational velocity of the orifice plate and the applied voltage is expressed by Eq. (2).

$$v_o = C_{vel} V \sin(\varpi t + \phi) \tag{2}$$

Where v_o is the velocity of the orifice plate, C_{vel} is the Proportionality constant, V is the amplitude of the applied voltage to the PZT, ω is the angular velocity, and ϕ is the phase difference between the applied voltage and the velocity of the orifice plate.
The amplitude of the vibrational velocity changes by the position on the orifice plate because the orifice plate is vibrated like a clamped circular plate. Therefore, the initial velocity of the particles v_{init} is expressed by Eq. (3)

$$v_{init} = C_{part} C_{vel} V \tag{3}$$

Where C_{part} is the Proportionality constant.
The forces acting on the particle is obtained from the pressure distribution around the particle, the drag force due to the working fluid, and the gravity force. The pressure distribution around the particle is divided into three areas as shown in figure 6. The pressures in the area shown in figure 6 (a) and (c) are the supplied pressure and the atmospheric pressure from the assumption (i), respectively. The pressure distribution in the area shown in figure 6 (b), which is the narrow flow path is obtained from the assumption (ii). The area is developed as figure 7. From the assumption (iii), the height of the flow path is the average value of it. From the figure 7, the surface of the sphere $h_p(r)$ and the average height of the flow path h_{ave} are expressed by Eq. (4) and Eq. (5).

$$h_p(r) = r_p + z_h \sin\alpha - \sqrt{r_p^2 - (r - r_p - z_h \cos\alpha)^2} \tag{4}$$

$$h_{ave} = \frac{\int_{r1}^{r2} h_p(r) dr}{r_2 - r_1} \tag{5}$$

Where r_p is the radius of the particle, z_h is the distance between the displacement of the particle based on the assumption (iv) and that of the valve seat based on the assumption (v), r_1 and r_2 are the distance to the lower edge and upper edge at the valve seat, and α is the half apex of the valve seat, respectively.
The flow in the area shown in figure 6 (b) is expressed by Navier-Stokes equations Eq. (6) in cylindrical coordinates with the assumption (ii) and (vi).

$$\frac{\partial P(r)}{\partial r} = \mu \frac{\partial^2 v_r(r,h)}{\partial h^2} \tag{6}$$

Where $P(r)$ is the pressure between the particle and the valve seat, μ is the dynamic viscosity of the working fluid, and $v_r(r, h)$ is the flow velocity in the r-axis direction, respectively.
The flow velocity $v_r(r, h)$ is derived from Eq. (6) with the boundary conditions shown in Eq. (7). The flow velocity is expressed by Eq. (8).

$$\begin{aligned} v_r(r,0) &= V_{r1} \\ v_r(r,h_{ave}) &= V_{r2} \end{aligned} \tag{7}$$

$$v_r(r,h) = \frac{1}{2\mu}\frac{\partial P(r)}{\partial r}(h^2 - h_{ave}h) + \frac{h}{h_{ave}}(V_{r2} - V_{r1}) + V_{r1} \tag{8}$$

Where V_{r1} and V_{r2} are the velocity of the valve seat and the particle in the r-axis direction, respectively.
The continuity equation in the cylindrical coordinates is expressed by Eq. (9) with the assumption (vi).

$$\frac{\partial v_r(r,h)}{\partial r} + \frac{v_r}{r} + \frac{\partial v_h(r,h)}{\partial h} = 0 \tag{9}$$

Where $v_h(r, h)$ is the flow velocity in the h-axis direction.
The pressure distribution $P(r)$ is derived by integrating Eq. (9) over h from 0 to h_{ave} and substituting Eq. (8) for it. The pressure distribution is expressed by Eq. (10).

$$P(r) = Ar^2 + Br + C_1 \log r + C_2$$
$$A = \frac{3\mu}{h^3}(V_{h2} - V_{h1}), B = \frac{6\mu}{h^2}(V_{r2} - V_{r1}) \tag{10}$$

Where V_{h1} and V_{h2} are the velocity of the valve seat and the particle in the h-axis direction, and C_1 and C_2 are constants of integration, respectively. C_1 and C_2 are derived from the boundary conditions shown in Eq. (11). C_1 and C_2 are expressed by Eq. (12).

$$P(r_1) = 0$$
$$P(r_2) = P_s \tag{11}$$

$$C_1 = \frac{1}{\log \frac{r_2}{r_1}}(P_s - A(r_2^2 - r_1^2) - B(r_2 - r_1))$$
$$C_2 = -Ar_1^2 - Br_1 - \frac{\log r_1}{\log \frac{r_2}{r_1}}(P_s - A(r_2^2 - r_1^2) - B(r_2 - r_1)) \tag{12}$$

Where P_s is a supply pressure.
The vertical force generated by pressure in the flow path F_{path} is derived from P (r) and the surface area of the particle in contact with flow path. F_{path} is expressed by Eq. (13).

$$F_{path} = \int_{r_1}^{r_2} P(r)\theta_c r dr \tag{13}$$

Where θ_c is the central angle in the developed view of the flow path. θ_c is expressed by Eq. (14).

$$\theta_c = 2\pi \sin \alpha \tag{14}$$

From the above, the resultant force acting on the particle due to the pressure F_P are expressed by Eq. (15).

$$F_P = (0 - \pi r_o^2 P_s) + (F_{path} - \int_{r_1}^{r_2} P_s \theta_c r dr) \tag{15}$$

The first term is the force due to the differential pressure between the pressure in the valve and the orifice, the second term is the force due to the differential pressure between the pressure in the valve and the flow path.
The drag force acting on the particle is used the Stokes drag shown as Eq. (16).

$$F_D = 6\pi\mu r_p v_p \tag{16}$$

Therefore, the acceleration of the particle a_p is expressed by the Eq. (17).

$$a_p = \frac{F_P + F_D \pm mg}{m} \tag{17}$$

The collision between the particle and the valve seat is expressed by Eq. (18) from the assumption (vii).

$$v_p' = v_o - ev_p + ev_o \tag{18}$$

Where e is the coefficient of the restitution, v_p and v_p' are the velocity of the particles before and after colliding with the orifice plate, v_o is the velocity of the orifice plate before and after colliding with the particles.

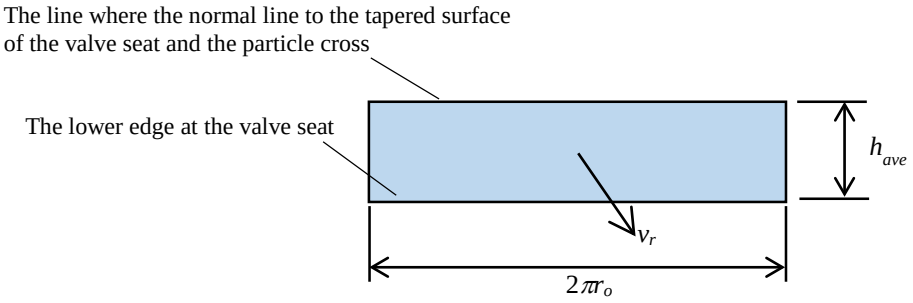

FIGURE 8. Area used for flow rate measurement

Flow between the particles and valve seat of the orifices

The flow rate is derived from the average of the instant flow rate flowing through the area shown in figure 8. The instant flow rate Q (t) is expressed by Eq. (19).

$$Q(t) = 2\pi r_o \int_0^{h_{ave}} v_r(r_1, h)dh \tag{19}$$

Therefore, the average flow rate Q_{ave} is expressed by Eq. (20).

$$Q_{ave} = \frac{\int_T Qdt}{T} \tag{20}$$

Where T is the period of the integration.

RESULTS OF THE NUMERICAL CALCULATION

We calculated the average flow rate by the numerical calculation, when the silicone oil shown in Table 1 was used as the working fluid under the applied pressure of 0.1 MPa to 0.5 MPa. The input parameters are shown in Table 2. The values obtained through the previous experiment were used as the applied voltage and the driving frequency in the simulation. The calculated results are shown in Table 3. The experiment was conducted to obtain the applied voltage which is required for flow of 5 ml/min. Most results with the kinematic viscosity value 1 mm^2/s show errors under 5% though 26.4% error occurred under 0.2 MPa. According to the increase of the kinematic viscosity, the results show large errors. It is considered that the increase of the error comes from the assumptions of (iii) in the previous section. Note that the calculated results were calculated by tripling the value obtained from Eq. (20) because there are three orifices arranged on the closest places from the center of the orifice plate.

TABLE 1. Condition used to calculate the average flow rate.

No.	**Kinematic viscosity [mm^2/s]**	**μ [×10^{-6} Pa·s]**	**ρ [kg/m^3]**
#1	1	818	818
#2	3	2610	869
#3	5	4480	897

TABLE 2. Model parameters for the numerical calculation.

Item	**Value**
r_p [mm]	0.4
α [rad]	π / 4
r_1 [mm]	0.283
r_2 [mm]	0.424
m [mg]	2.11
T [s]	1
C_{vel}	0.0074
C_{part}	0.984
e	0.65

TABLE 3. Calculated flow rate and errors comparing its value and the experimental results.

Kind of the working fluid	P_s [MPa]	Q_{ave} [ml/min]	Error [%]
#1	0.1	4.94	1.2
	0.2	3.68	26.4
	0.3	4.89	2.2
	0.4	4.93	1.4
	0.5	5.23	4.6
#2	0.1	24.2	384
	0.2	23.3	366
	0.3	14.5	190
	0.4	10.3	106
	0.5	9.59	91.8
#3	0.1	115	2200
	0.2	33.4	568
	0.3	20.2	304
	0.4	12.4	148
	0.5	10.5	110

DISCUSSION AND CONCLUSION

In this paper, an analytical model considering the motion of the particle and the flow rate was proposed, when the particles are near the orifices. We compared the analytical results and the experimental results. The errors between the calculation results and the experimental results were maximum 26.4% and minimum 1.2%, when the silicone oil was used as the working fluid with the kinematic viscosity value 1 mm^2/s. From the results, we verified the validity of the analytical model with the low viscosity fluid. However, the increase in the dynamic viscosity of the working fluid caused the larger error in the flow rate. This is due to the assumptions that the relationship between the particles and the valve seat of the orifices are regarded as a parallel plate. This hypothesis causes the difference of the pressure distribution, which gives larger effects in the results with the higher kinematic viscosity. Therefore, an improved model considering the spherical shaped flow path should be developed to obtain reasonable results under larger viscosity in future work.

ACKNOWLEDGMENTS

This research was funded by ImPACT Program of Council for Science, Technology and Innovation (Cabinet Office, Government of Japan).

REFERENCES

1. Raibert, M., Blankespoor, K., Nelson, G., Playter, R., et al., BigDog, the Rough-Terrain Quadruped Robot, Proceedings of the 17th World Congress, Vol. 17, No. 1, 2008, p. 10822–10825.
2. Semini, C., Tsagarakis, N. G., Guglielmino, E., Focchi, M., Cannella, F., Caldwell, D. G., Design of HyQ - a Hydraulically and Electrically Actuated Quadruped Robot, Proceedings of the Institution of Mechanical Engineers, Part I: Journal of Systems and Control Engineering, Vol. 225, No. 6, 2011, p. 831–849.
3. Jiaqi, Z., Feng, G., Xiaolei, H., Xianbao, C., Xueying, H., Trot Gait Design and CPG Method for a Quadruped Robot, Journal of Bionic Engineering, Vol. 11, No. 1, 2014, p. 18–25.
4. Plummer, A., Electrohydraulic Servovalves -Past, Present, and Future, 10th International Fluid Power Conference, IFK2016, 2016.
5. Ukida, T., Suzumori, K., Nabae, H., Kanda, T., Ofuji, S., Hydraulic Control by Flow Control Valve Using Particle Excitation, Transactions of the Japan Fluid Power System Society, Vol. 47, No. 6, 2016, p. 39–46 [in Japanese].
6. Hirooka, D., Suzumori, K., Kanda, T., Flow Control Valve for Pneumatic Actuators Using Particle Excitation by PZT Vibrator, Sensors and Actuators A: Physical, Vol. 155, No. 2, 2009, p. 285–289.
7. Hirooka, D., Yamaguchi, T., Furushiro, N., Suzumori, K., Kanda, T., Speed Control of Pneumatic Cylinder using Particle-Excitation Flow Control Valve, Transactions of the Japan Fluid Power System Society, Vol. 46, No. 2, 2015, p. 7–13 [in Japanese].